UNIVERSITY OF OKLAHOMA GRADUATE COLLEGE

EXPERIMENTAL ANALYSIS AND OPTIMIZATION OF BATTERY THERMAL MANAGEMENT SYSTEMS

A THESIS

SUBMITTED TO THE GRADUATE FACULTY

In partial fulfillment of the requirement for the

Degree of

Master of Science

By TOAN MATSUMOTO

Norman, Oklahoma

2025

EXPERIMENTAL ANALYSIS AND OPTIMIZATION OF BATTERY THERMAL MANAGEMENT SYSTEMS

A THESIS APPROVED FOR THE
SCHOOL OF AEROSPACE AND MECHANICAL ENGINEERING

BY THE COMMITTEE CONSISTING OF

Dr. Zhang Dong, Chair

Dr. Merchan-Merchan Wilson

Dr. Xu Bin

Table of Contents

List of Figures

List of Tables

Abstract

Batteries have become vital to daily life, with demand increasing due to the widespread adoption of electric vehicles. As battery usage expands, ensuring safe and efficient operation is crucial. A key challenge is the gradual degradation of cell capacity, which accelerates over repeated charge and discharge cycles. Factors such as charging rates, ambient conditions, and excessive heat generation significantly impact battery longevity. In high-power applications like EVs, rapid charging and discharging can elevate cell temperatures beyond recommended limits, leading to increased degradation and potential safety risks, making the battery pack unusable.

This study investigates various cooling strategies to regulate lithium-ion cell temperatures and prevent excessive heat buildup. By charging cells at different C-rates and continuously monitoring surface temperatures in a battery pack, the effectiveness of passive and active cooling mechanisms in preventing thermal runaway and uniform cell temperature is evaluated. Additionally, the study explores water cooling and PCM-based thermal regulation, analyzing their impact on temperature stability. The results provide insights into battery thermal management optimization, enhancing both safety and longevity in EVs and other high-demand applications.

Furthermore, using the experimentally collected data, a thermal model is developed to predict temperature behavior during the charge cycle of a single cell. This model serves as a foundation for future improvements in battery pack thermal modeling, allowing for more accurate simulations and optimized cooling system designs. The findings contribute to the advancement of Battery Thermal Management Systems, ensuring reliable and efficient performance in next-generation energy storage solutions.

Introduction

As the problem of global warming increases, the demand for renewable energy sources and efforts to decrease greenhouse gases, mainly carbon dioxide (CO_2) and methane (CH_4), emitted into the atmosphere by burning fossil fuels also increases [1]. Over the past few decades, scientific research has highlighted how rising global temperatures, melted ice caps, and shifted weather patterns are tied to increasing levels of greenhouse gases in the atmosphere. These findings have pushed governments, industries, and communities worldwide to seek sustainable alternatives to conventional fossil fuels, aiming to reduce emissions and slow the pace of climate change.

One of the largest sources of these greenhouse gases is the transportation sector [2]. This sector includes a variety of vehicles, from personal cars and motorcycles to buses and trucks. Most of these rely heavily on internal combustion engines, which burn gasoline or diesel and release significant amounts of carbon dioxide and other pollutants into the air. To reduce the number of these conventional vehicles, many countries have implemented efforts to promote and increase the use of electric vehicles (EVs) [3]. In many cases, these initiatives involve policy changes such as tax incentives, subsidies, and investments in public charging infrastructure to encourage consumers to adopt cleaner modes of transportation.

Electric vehicles are vehicles that use an electric motor and battery instead of a gasoline- or diesel-powered engine [4]. Due to the absence of an internal combustion engine, EVs do not emit any greenhouse gases while operating. This key difference is often viewed as a major advantage in the global effort to reduce carbon emissions and reliance on fossil fuels. Although it may sound simple to replace all internal combustion vehicles with electric vehicles, many challenges must be addressed for this transition. Adopting EVs on a massive scale calls for the expansion of charging facilities, improvements in battery technology, and the development of more efficient power grids capable of handling the increased electricity demand.

Although they have many advantages, there are still drawbacks and problems that must combated. These include charging infrastructure, battery life, cost of repairs, and the waste generated by these batteries [5]. For instance, many regions still lack sufficient fast-charging stations to make EV travel convenient, and the process of replacing or disposing of high-capacity lithium-ion batteries remains complex and costly. Moreover, while electricity used to power EVs can come from renewable sources, it can also come from fossil fuels, highlighting a broader need to decarbonize electricity generation as well.

To tackle these issues, a common method is to improve the battery thermal management systems (BTMS) in these EV battery packs. A BTMS regulates the temperature of a battery pack by actively cooling or heating it, allowing the battery to operate within its optimal temperature range. The temperature of these battery packs is crucial, as it is correlated with degradation, performance, range, and even safety [6]. For example, when batteries overheat, their chemical reactions accelerate, leading to faster degradation of battery cells and a reduction in overall lifespan. Poor BTMS design can lead to premature battery degradation, reduced driving range, and even thermal runaway, where the battery overheats and can catch fire.

As the demand for safer and longer-lasting batteries increases, there has been extensive research conducted on Battery Thermal Management Systems. Various cooling mechanisms have been proposed and studied, each with its unique strengths and limitations. Conventional systems such as air and liquid cooling are straightforward to implement, but this may not always provide the temperature uniformity or thermal buffering necessary for high-demand applications like electric vehicles (EVs). In contrast, Phase Change Materials (PCMs) have gained increasing attention due to their latent heat storage capabilities, which can significantly delay temperature rise during operation.

PCM-based systems absorb thermal energy during the phase change process, allowing for passive control of temperature spikes without consuming additional energy. Maknikar and Pawar presented a critical review of PCM applications in BTMS, outlining how factors such as material selection, thermal conductivity, and geometric configuration play vital roles in system efficiency [7]. However, they also emphasized that the inherently low thermal conductivity of PCMs limits their long-term effectiveness.

Dinker explored organic PCM materials, noting their benefits over traditional inorganic counterparts. Organic PCMs are non-corrosive, chemically stable, and environmentally safe, making them more suitable for EV battery applications [8].

Recent studies have reinforced this hybrid approach. For example, Zhang numerically investigated how thermophysical properties of PCM—including melting point, thermal conductivity, and latent heat—affect BTMS performance [9]. Their findings confirmed that misalignment between PCM properties and cell heat generation profiles can lead to suboptimal performance. Moreover, comparative studies have shown that while PCMs are effective in reducing peak temperatures, their thermal saturation point can hinder continued heat absorption during prolonged or repeated cycles.

To address these limitations, hybrid BTMS designs that combine PCMs with active cooling have been proposed. These systems aim to leverage PCM's energy absorption capacity while using airflow or coolant circulation to improve heat dispersion. PCM-cooled systems have also shown a potential to outperform traditional methods in both thermal balance and energy efficiency, especially in EV settings [10].

In addition to maintaining temperature within safe operating ranges, minimizing cell-to-cell and intra-cell temperature differences is critical for battery longevity. Li found that even a 3 °C temperature variation across a cell can accelerate degradation by up to 300%, primarily due to uneven current distribution and localized overpotentials [11]. Rüwald further demonstrated experimentally that in parallel-connected cells, elevated thermal gradients result in uneven aging, voltage imbalance, and compromised pack performance over time [12].

These studies emphasize the need for BTMS designs that not only prevent overheating but also promote thermal uniformity. While PCMs are effective at dampening rapid temperature increases, their spatial thermal conductivity is often insufficient for managing these internal gradients—hence the need for hybrid systems or design optimization.

To design more efficient BTMS configurations, researchers have increasingly turned to computational optimization methods. Particle Swarm Optimization (PSO) has proven effective for BTMS design.

For example, Liu applied PSO to optimize an air-liquid coupled BTMS, achieving a reduction in maximum cell temperature and improving temperature uniformity [13].

PSO has also been used to tune thermal control strategies. Sayah developed a PSO-based thermal control system for hybrid electric vehicle energy systems [14]. The algorithm dynamically adjusted system parameters to maintain ideal battery temperature ranges under variable driving conditions. The reviewed literature highlights the significant impact of PSO in advancing BTMS design and control strategies, reinforcing its growing application in both academic and industrial battery research.

While significant advancements have been made in battery thermal management using PCM and PSO-based optimization, several key gaps remain in the existing literature. Most experimental studies focus on either single-cell testing or fully commercialized cooling systems, with limited attention paid to custom-built battery packs assembled from scratch, especially in configurations like 1S3P. Additionally, although many works have demonstrated the effectiveness of PCMs in reducing peak cell temperature, few have examined their ability to reduce cell-to-cell thermal heterogeneity—a crucial factor influencing pack degradation and safety. Hybrid cooling systems have been proposed in simulation but lack extensive experimental validation on small-scale modular packs.

This thesis addresses these gaps through a combined experimental and computational approach. First, a custom-designed 1S3P battery pack was physically assembled and tested under varying C-rates using multiple cooling configurations, including no cooling, PCM, and hybrid PCM-water cooling. This setup allows for direct measurement of cell-to-cell temperature differences, enabling evaluation of cooling effectiveness not just in peak suppression, but also in thermal uniformity. Second, a physics-based lumped thermal model was developed for the charging process of a single 18650 cell, and its parameters were optimized using Particle Swarm Optimization (PSO). Unlike many existing models, this was directly validated using experimental surface temperature data collected from physical tests. By doing so, this work not only improves understanding of cooling strategies at the pack level but also bridges simulation and real-world testing using an optimization-driven modeling framework.

System Requirement and Conceptual Design

Battery Cells

Batteries come in a wide range of types and configurations, each designed for specific applications. They may differ in terms of chemistry, voltage rating, maximum current, and optimum operating temperature. In this experiment, the nickel–cobalt rechargeable (NCR) batteries manufactured by Panasonic, commonly referred to as NCR 18650B cells, will be utilized [15]. These cells are widely employed in devices such as laptops, power tools, and electric vehicles because of their high energy density, reliability, and long lifespan [16]. However, their high energy density also makes them prone to explosion if they are overcharged or over-discharged under undesired conditions.

NCR 18650B cells are cylindrical in shape, measuring 18 mm in diameter and 65 mm in height, with the positive terminal at one end and the negative terminal at the other, as shown in Figure 1. Each cell has a capacity of 34000 mAh, a maximum voltage of 4.2 V, and a minimum voltage of 2.5 V. The nominal voltage of 3.6 V is considered optimal for storage [17]. For safety, the recommended maximum charge and discharge current is 4.87 A—approximately 1.48 C—where 1 C is defined as the current required to fully charge the cell from its minimum voltage in one hour.

Figure 1: NCR 18650B Cells [18]

When cycling these batteries, it is essential to ensure that operating conditions remain within established safety limits. As previously mentioned, each cell is rated to operate at a specific C-rate. In electric vehicles, the C-rate can vary significantly depending on driving conditions. For instance, when a vehicle is cruising on a flat surface, the C-rate may be as low as 0.2C, whereas, during acceleration on an incline, it can increase to around 2C [6]. Higher charge and discharge rates generally result in elevated cell temperatures due to the chemical reactions occurring within the battery, which involve the transfer of ions between the cathode and anode. According to the manufacturer's specifications, the optimum charge and discharge temperature range for NCR cells is between 0°C and 45°C [17]. Maintaining battery operations within these parameters is crucial for safety, performance, and longevity.

Battery Pack Assembly

When multiple cells are incorporated into a system, they may be arranged in series or parallel configurations. In electric vehicles, battery packs typically contain around 3000 NCR 18650 cells, although in Tesla's Model X and Model S, the number can exceed 8200 cells [19]. The configuration of these cells has a significant impact on the overall characteristics of the assembled battery pack. When cells are connected in series, their voltages add together while the total capacity remains the same. Conversely, when connected in parallel, the voltage remains constant, but the total capacity is the sum of the individual cells. As illustrated in Figure 2, a single module can consist of 444 cells arranged in a 6S74P configuration (6 in series and 74 in parallel). This configuration provides a nominal voltage of 22.8 V and can support discharge currents of up to 750 A [20].

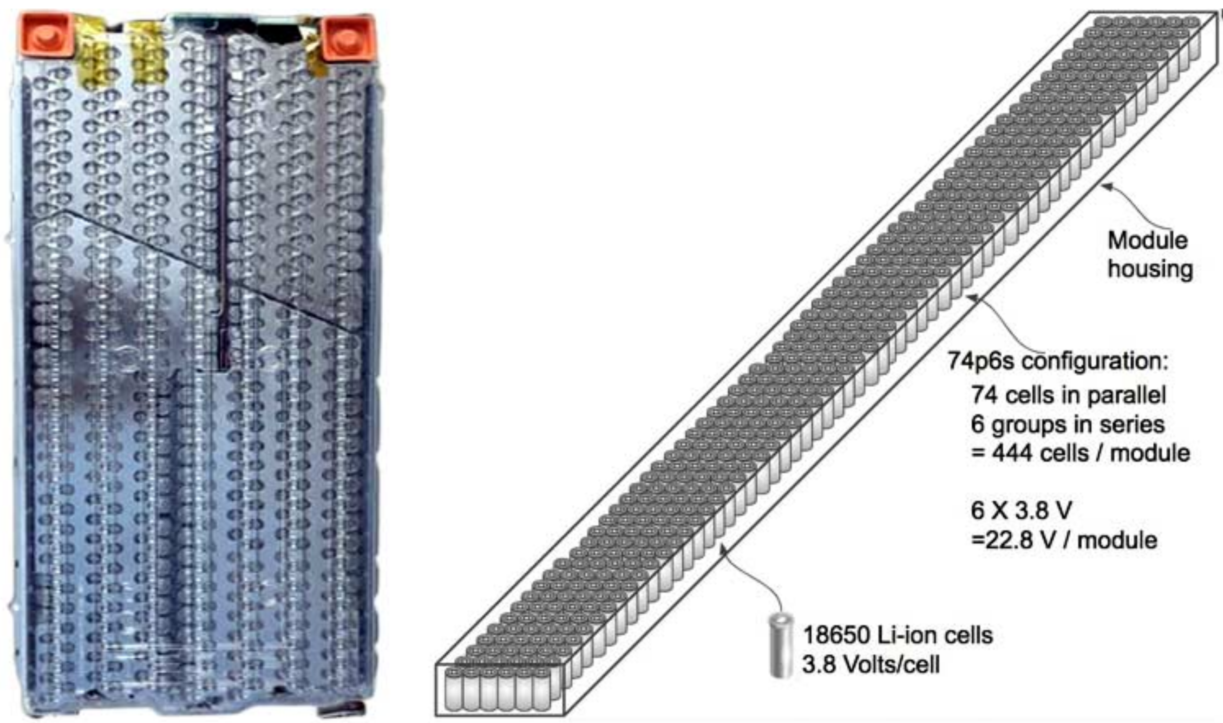

Figure 2 Tesla model-S Battery Module [21]

To connect the cells in series or parallel configurations, nickel strips are typically spot welded to the cell terminals, as illustrated in

Figure 3. Nickel strips are widely used in battery pack assembly due to their high electrical conductivity, excellent corrosion resistance, and ease of spot welding [22]. This approach enables

the assembly of cells into a variety of configurations and shapes to meet specific design requirements.

Figure 3 - Sport Welded Cell [23]

Cooling Mechanisms

As discussed, maintaining the optimal temperature of batteries is critical for ensuring both their longevity and efficiency. Research on battery thermal management systems has become a major focus within the electric vehicle industry. Significant resources have been invested in identifying the most effective methods for regulating battery temperatures during operation. The three most common BTMS approaches are air cooling, phase-change material (PCM) cooling, and liquid cooling [24]. Air cooling involves using fans or natural convection to circulate air around the battery cells, thereby dissipating heat. It is a relatively easy and cheap solution, but there is a limited cooling capacity compared to other methods. PCM cooling employs materials capable of absorbing and releasing thermal energy through phase transitions; for example, when a PCM transitions from a solid to a liquid, it absorbs heat [25]. Due to the high latent heat capacity, PCMs can effectively extract heat from cells and help maintain a relatively constant battery pack temperature. On the other hand, a constant cycle of solidifying and melting can wear the material out and engineers must make sure the PCM does not leak out of the battery module when it is in the liquid phase [26]. Finally, liquid cooling is another widely used method, where a coolant is circulated through the battery pack to reduce overall temperature within the battery pack [27]. The coolant mechanism allows engineers to precisely control the temperature of the module, but this adds more parts such as a pump, and reservoir, which ultimately adds to the complexity of the system.

Battery Testing

In this study, two battery testing systems are employed to evaluate both individual cells and battery packs. Single-cell testing is conducted using a Neware CT-4008T battery tester, which provides precise control over charge and discharge currents while simultaneously measuring cell voltage and surface temperature via a K-type thermocouple. For battery pack testing, an Arbin battery tester is utilized, which operates like the Neware. Both machines regulate the input current and measure voltage and temperature using K-type thermocouples. In addition, both testing systems include built-in safety features, allowing the configuration of voltage cutoffs, current limits, and maximum operating temperatures, thereby preventing overcharging, undercharging, and overheating. These safeguards ensure that testing procedures adhere to recommended safety standards and yield reliable performance data for both cells and battery packs.

Experimental Procedure

Setting the test schedule file

To test the battery cells and pack, a schedule file must be created using the Arbin MTS 8.0 software. This software allows precise control over the charging and discharging parameters by allowing users to define input parameters such as current. The schedule file can be configured to charge the cells at various C-rates until a specified voltage threshold is reached. Additionally, the software supports real-time monitoring and data acquisition, with up to 12 voltage measurement channels with a minimum resolution of 0.0001 volts and 12 thermocouples. This allows for comprehensive tracking of both electrical and thermal behavior, ensuring accurate performance analysis and validation of the battery thermal management system.

Single cell setup

The single-cell testing was conducted using a Neware battery cycler under controlled ambient laboratory conditions. To ensure consistency across all thermal configurations, a custom acrylic enclosure was designed to house a single 18650 cell. This enclosure maintained a fixed internal volume and provided uniform external boundary conditions across tests. It was constructed using 0.25-inch thick acrylic sheets, which were laser-cut for precision and bonded using acrylic adhesive to form a rigid, sealed structure.

Each test cell was connected to an individual Neware channel. The baseline test, with the cell exposed to ambient air, was carried out using slot 7, while the cell embedded in phase change material (PCM) was tested in slot 8 of the Neware holder. In both cases, a K-type thermocouple was secured to the center of the cylindrical surface of the cell using high-temperature-resistant tape, allowing for accurate surface temperature monitoring throughout the charge-discharge cycles [28].

For the PCM configuration, the cell was fully encapsulated in PCM within the same acrylic enclosure. The PCM material used in this study was generously provided by Dr. Givtesh Garg, who also performed the filling process to ensure uniform distribution and proper thermal contact around the cell. This setup facilitated a direct performance comparison between the air-cooled and PCM-cooled configurations, under identical electrical cycling conditions and structural constraints.

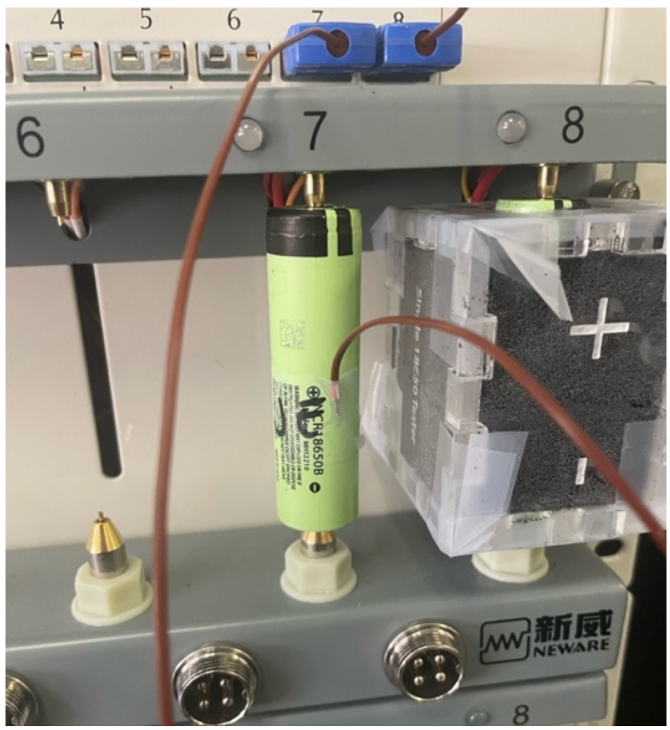

Figure 4 - Single Cell Testing.

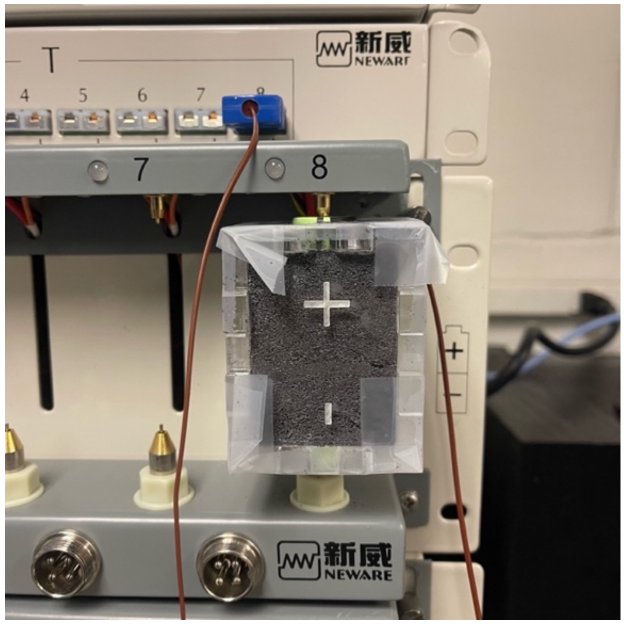

Figure 5 Single Cell Embedded in PCM

Pack setup

To arrange and secure the cells, a custom acrylic casing was designed for a battery pack configuration with 3 cells in parallel connection. The casing has a 5 mm gap between each cell and between the cells and the casing walls, a common standard for PCM applications [29]. Figure 7

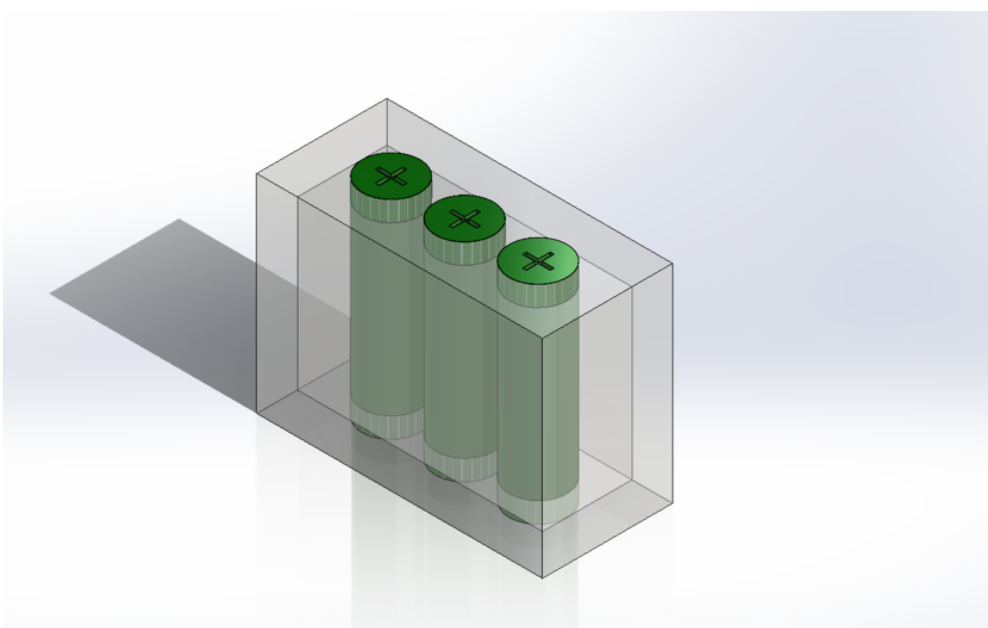

Figure 6 1S3P CAD Design

illustrates the computer aided design model of the three cells positioned in the same orientation, allowing their terminals to be connected via a nickel strip. In this 1S3P setup, the pack's maximum voltage is 4.2 V, nominal voltage is 3.6 V, and cutoff voltage is 2.5 V. Connecting three cells in parallel provides a total capacity of 10.05 Ah (10,050 mAh). Charging at 0.5C requires 5.025 A, at 1C requires 10.05 A, and at 1.5C requires 15.075 A.

Figure 7 - 1S3P 18650 Design

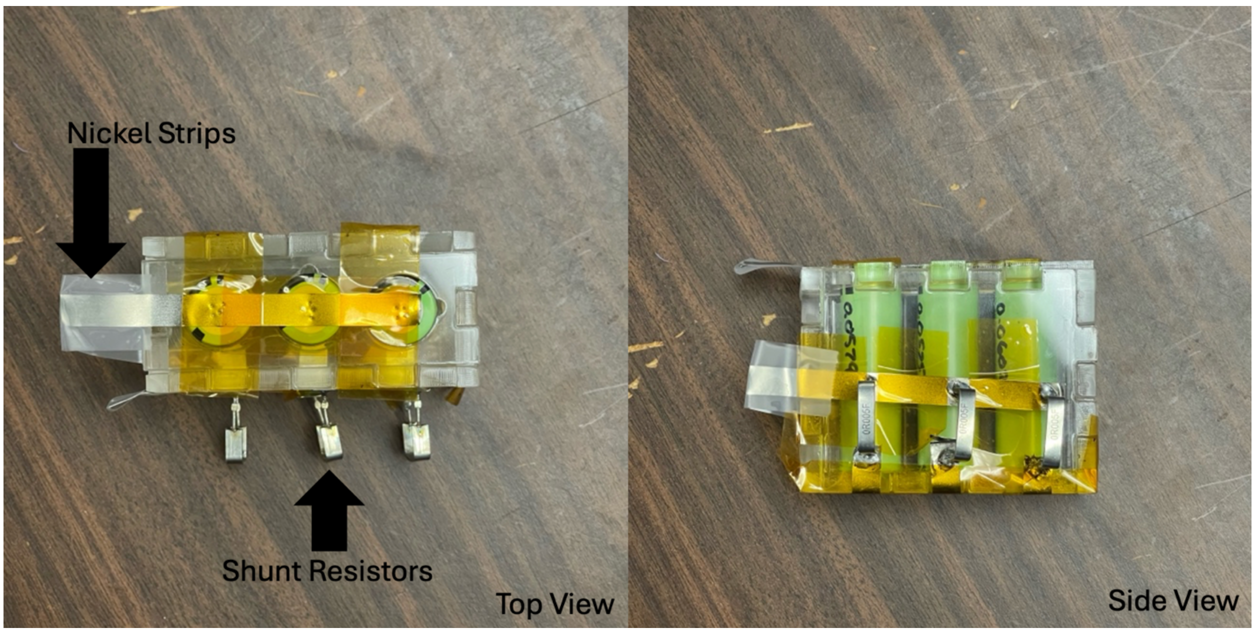

Figure 8 - 1S3P 18650 Pack with no cooling mechanism

As noted previously, each cell terminal is connected using a nickel strip. Nickel is commonly used in industry due to its high electrical conductivity and its relative ease of spot welding. For this pack assembly, a 5 mm wide nickel strip and a standard off-the-shelf spot welder were used to ensure electrical connections between the cells. A k-type thermocouple is placed on the center of the surface of each cell to monitor the temperature during the cycles.

\

Figure 9 - Spot welder and Nickel Strip Used

Use of Shunt Resistors

One limitation of the Arbin battery tester is that it does not provide a direct method for measuring the current flowing through each cell in a battery pack. While the system can accurately measure the total pack current and voltage, obtaining cell-level current data is necessary for a more detailed analysis of individual cell behavior is necessary. Theoretically, each cell should receive an equal share of the total current. However, due to variations in internal resistance caused by manufacturing inconsistencies and aging some cells will slightly receive current than others. These imbalances can lead to uneven heating, accelerated degradation, and reduced overall pack efficiency.

To overcome this limitation, shunt resistors were implemented. Shunt resistors are low-value precision resistors placed in series with each cell, allowing for indirect current measurement. By measuring the voltage drop across these resistors and applying Ohm's Law in Equation 1, the current flowing through each cell can be determined. This method enables real-time monitoring of current distribution, providing insight into potential imbalances and allowing for further optimization of battery pack design and thermal management strategies.

$$Current_{shunt} = \frac{Voltage_{shunt}}{Resistor_{shunt}} \quad (1)$$

Since the shunt resistors are placed in series with each cell, it can be assumed that the current flowing through each shunt resistor is identical to the current flowing through the corresponding cell. The Arbin battery tester is equipped with an auxiliary measurement box, that can measure voltage with a resolution of 0.001 V. Given that each cell is expected to receive at least 1.675 A when charged at 0.5C, the required shunt resistance can be determined using Ohm's Law,

$$Resistor_{shunt} = \frac{Voltage_{shunt}}{Current_{shunt}} \quad (2)$$

Using the ohms law, the minimum resistance needed to suffice the minimum was 0.000597 ohms. As seen in the equation below. Therefore, the shunt resistor chosen for this pack will have a resistance of 0.005 Ω.

$$V = IR = 1.675A \times 0.005\Omega = 0.008375\text{V} \quad (3)$$

This voltage drop is above the 0.001 V resolution of the Arbin system, ensuring that the current measurements are detectable and accurate, as shown in equation 3. This proves we can use a shunt resistor with a resistance of 0.005 Ohms to accurately measure the current through each cell.

Cooling setup for 1S3P with PCM

For the setup with the battery pack filled with PCM, the cells were first inserted into the acrylic casing, with the thermocouple attached, then filled with PCM. This allowed the thermocouple to not be disrupted and be placed in the desired location. Once the PCM was filled, the lid was closed, and nickel strips were welded on. Figure 10 shows the final pack of the 1S3P pack filled with PCM ready for testing.

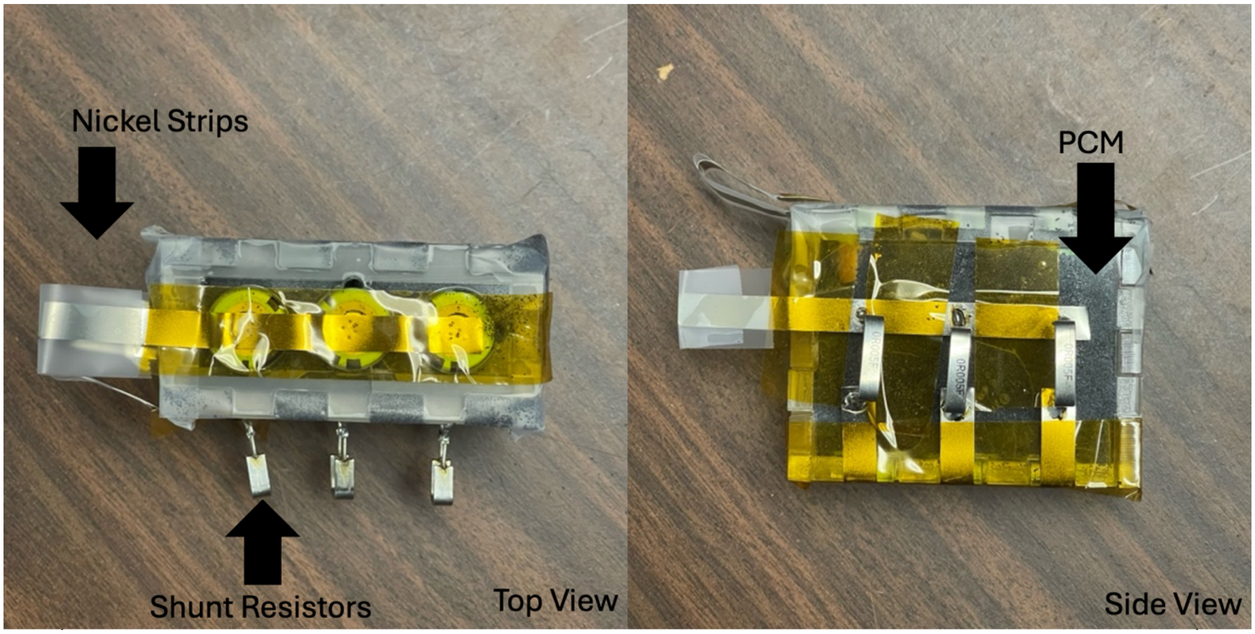

Figure 10 - 1S3P Pack with PCM

Cooling setup for 1S3P with Hybrid Cooling

The hybrid cooling configuration, which combined both phase change material and liquid cooling, required planning and careful execution due to its increased complexity. To begin, a schematic of the entire system was drafted prior to any physical assembly. This schematic was essential for determining the optimal routing of the cooling lines and ensuring the physical integration of components could be accomplished without compromising flow or structural integrity.

The primary objective of the schematic design was to minimize the total length of tubing used in the system while maintaining full coolant coverage over the battery pack. Reducing the tubing length not only improved system efficiency by minimizing pressure losses but also helped streamline the layout within the confined lab testing space. In addition, the routing had to be carefully planned to avoid sharp bends and potential kinking in the tubing, which could obstruct coolant flow or lead to long-term reliability issues.

As shown in Figure 11, the flow path for the coolant was designed to move linearly across the surface of the pack and exit through an outlet on the opposite side. This layout ensured continuous coolant movement while avoiding interference with the thermocouple wires and battery terminals. The coolant used was 1 liter of Thermaltake T1000 Pure Clear, circulated using a compact, low-noise electric pump [30]. Soft silicone tubing was selected for its flexibility, ease of sealing, and chemical compatibility with glycol-based coolants.

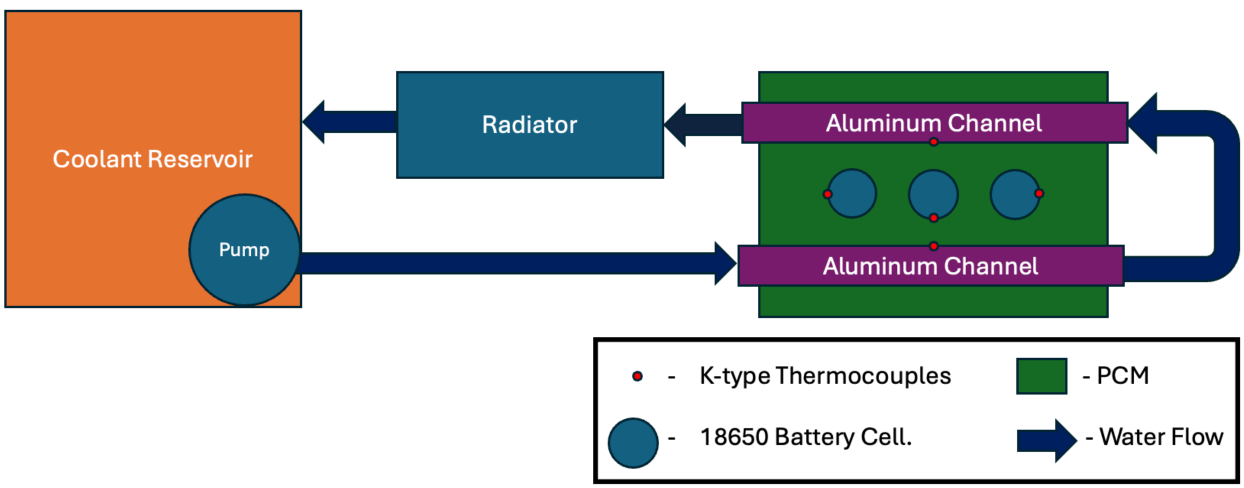

Figure 11 - Diagram of Hybrid Cooled Battery Pack

Figure 12 shows the hybrid-cooled 1S3P battery pack setup, illustrating the increased complexity compared to the PCM configuration. Because this system involves flowing coolant, the experimental apparatus was placed on the floor to prevent any potential spills from contacting the battery tester. The coolant contains less than 6% glycol—an additive commonly employed in industrial-scale BTMS applications [31]. The whole bottle of 1000ml was used in the system to ensure there was adequate amount in the reservoir.

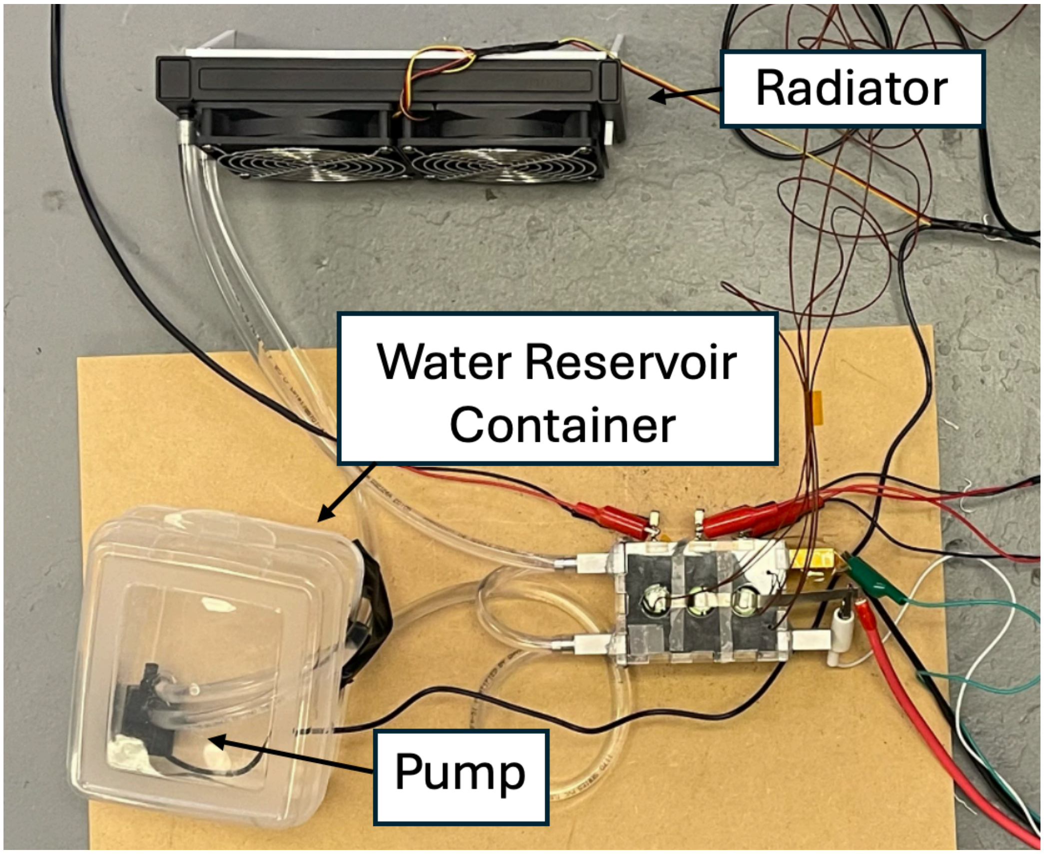

Figure 12 - 1S3P Pack with PCM and Water Cooling

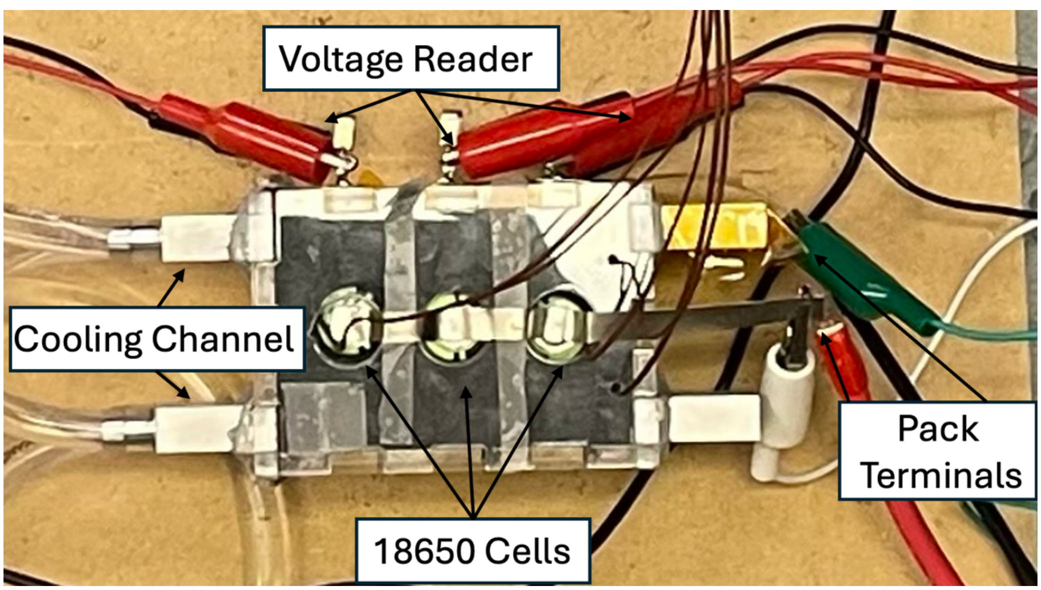

Figure 13 – Close-up picture of the PCM and Water-cooling pack

Testing Precautions

During the testing cycle and handling of the cells, it is important to follow strict safety procedures to mitigate potential risks. As previously mentioned, battery cells can result in electric shock, thermal runaway, or even an explosion. To prevent this, several safety protocols were implemented throughout the testing process. When not in use, the cells were stored in a refrigerator to maintain stability and minimize self-discharge. Individual cells were kept in their original manufacturer-provided casings to prevent physical damage, which could compromise the integrity of the cell.

For battery packs, where terminals are exposed, electrical tape was used to insulate the connections and reduce the risk of accidental short circuits. During testing, at least one person was always present in the lab to monitor the process and respond promptly to any unexpected events. High-current tests, particularly at 1.5C, were closely supervised to detect any signs of overheating or irregular behavior. These precautions ensured a controlled and safe experimental environment while minimizing the risks associated with high-energy battery testing.

Single Cell Testing Results

The first test conducted was an 18650 single-cell test in ambient air with no cooling mechanisms. This test was aimed at understanding the basic thermal behavior of the 18650 cell. The cell was inserted into Neewer slots and charged and discharged at three different C rates with no cooling mechanism. Table 1 below shows the test schedule that the cell underwent.

Table 1 18650 Single Cell Test Schedule

Step		until
1	Discharge @ 0.2C	2.5 V
2	Rest	30 mins
3	Charge @ 0.5C	4.2 V
4	Rest	30 mins
5	Discharge @ 0.5C	2.5 V
6	Rest	30 mins
7	Charge @ 1C	4.2 V
8	Rest	30 mins
9	Discharge @ 1C	2.5 V
10	Rest	30 mins
11	Charge @ 1.5C	4.2 V
12	Rest	30 mins
13	Discharge @ 1.5C	2.5V
14	Rest	30 mins
15	Charge 0.2C	3.6 V

Figure 14 presents the measured current, voltage, and temperature as a function of time. A key observation from the data is that higher C-rates result in greater temperature increases. When the cell was charged and discharged at 0.5C, the temperature increased from ambient conditions to approximately 28–31°C. At 1C, the temperature rose to approximately 33–37.5°C, while at 1.5C, the temperature increased further to 38–41°C. This observation aligns with findings in [32], where the cell temperature at different C rates was measured.

At each C-rate, the temperature during the discharge cycle is consistently higher than during the charging cycle. Furthermore, the temperature profile follows distinct trends, with the temperature increase during charging exhibiting a logarithmic pattern, whereas the temperature profile during discharge follows a sigmoid trend.

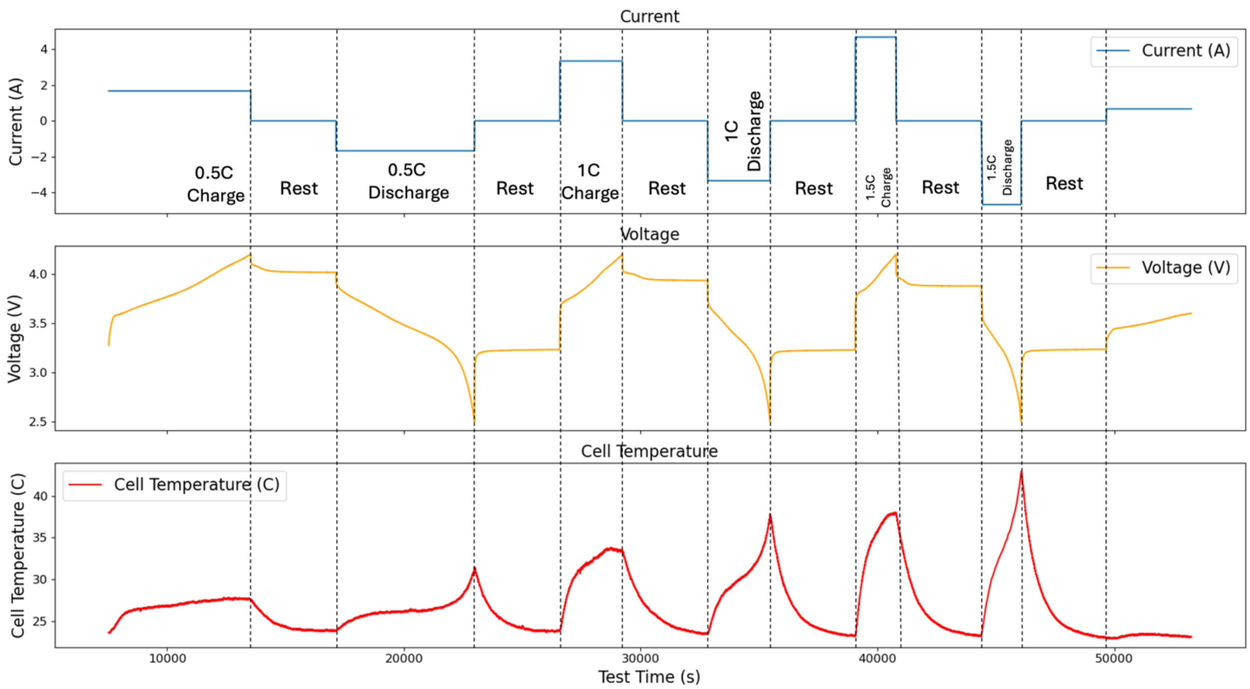

Figure 14 - 18650 Single Cell Test

Next, the single cell was then inserted into a casing filled with PCM. The identical test schedule as Table 1 was used.

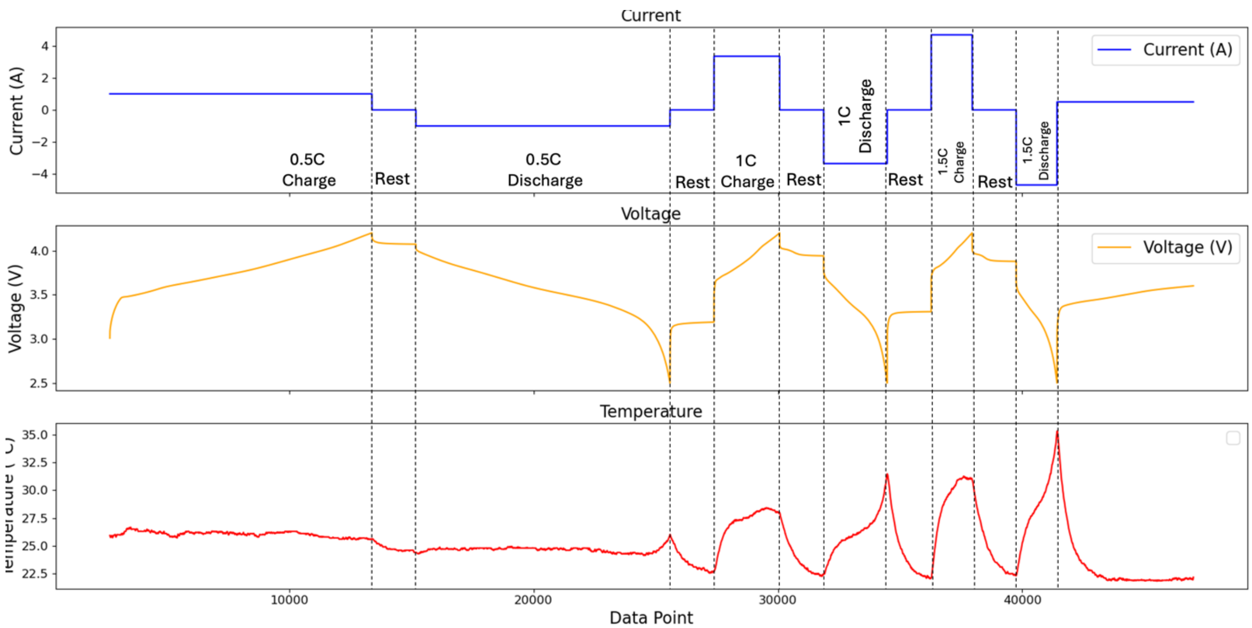

Figure 15 - 18650 Single Cell in PCM Test

From the temperature profile of the cell shown in Figure 15, it is evident that the use of PCM effectively mitigated the surface temperature rise during the charging and discharging cycles. The cell temperature peaked at 26°C, 32°C, and 37°C for 0.5C, 1C, and 1.5C rates, respectively. This demonstrates that the PCM effectively absorbed and dissipated heat, preventing excessive temperature increases, particularly during higher C-rate operations.

When compared to the cell without PCM, the temperature difference reached up to 3°C, signifying a substantial improvement in thermal management. The uncooled cell exhibited more pronounced temperature spikes, whereas the PCM-regulated cell maintained a more controlled and gradual temperature rise. This difference highlights the thermal buffering capability of PCM, which helps delay and moderate peak temperatures by absorbing latent heat during phase transition.

These findings confirm that PCM is an effective passive cooling solution for enhancing battery thermal stability, reducing temperature gradients, and minimizing the risk of thermal runaway. However, at higher C-rates (1.5C), the PCM approaches its thermal capacity, as seen in the increasing peak temperatures. This suggests that while PCM alone provides significant temperature regulation, integrating additional cooling mechanisms could further optimize the BTMS.

1S3P Pack Testing Results

Next, three 18650 cells were connected in parallel to form a 1S3P battery pack and tested. To monitor the performance of individual cells within the pack, a thermocouple and shunt resistor were attached to each cell in series, allowing real-time measurement of both temperature and current in individual cells. The cells were labeled with Cell 1 positioned closest to the pack's terminal, Cell 2 in the middle, and Cell 3 the furthest.

To evaluate the effectiveness of each cooling configuration, a controlled charge and discharge cycle was performed on the 1S3P battery pack at a constant 1C rate. This testing condition was deliberately selected to generate a substantial amount of heat within the pack, thereby simulating a moderately demanding operational scenario. The elevated thermal load allowed for a clear comparison between the different cooling strategies—no cooling, PCM-cooled, and hybrid PCM with water cooling. By maintaining the electrical input consistent across tests, the thermal performance of each setup could be assessed under identical conditions, providing insight into how effectively each system managed temperature rise and distribution within the battery pack.

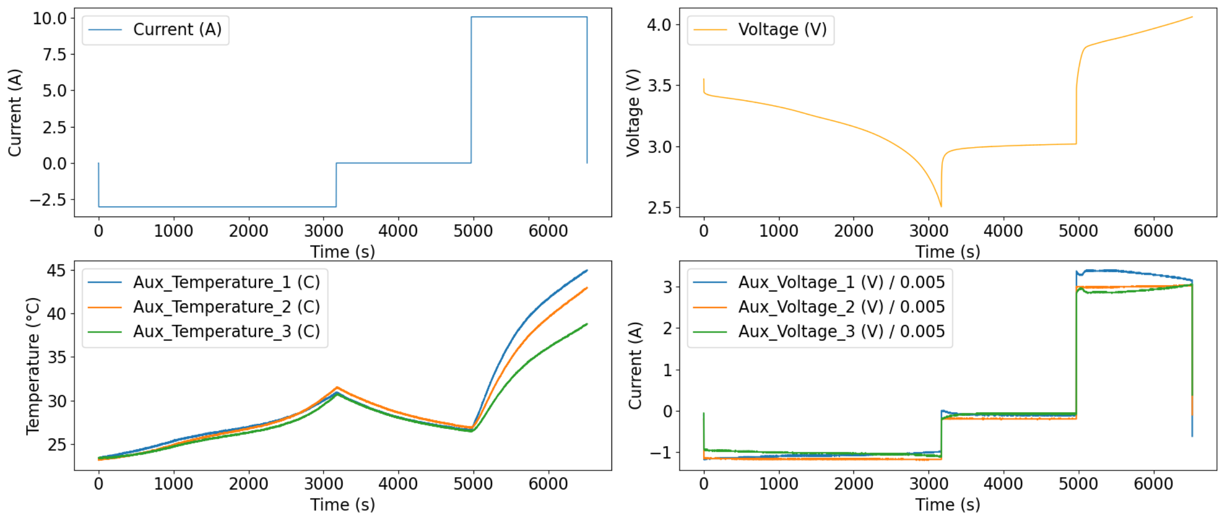

Figure 16 - 1S3P No Cooling Test

The initial test, conducted on the 1S3P battery pack without any cooling mechanism, showed a rapid temperature increase, ultimately reaching the safety cutoff at 45°C before completing a single full charge-discharge cycle. Without any thermal management mechanisms, the cells were unable to dissipate the heat generated during high C-rate operation, leading to thermal runaway conditions that forced the test to shut down.

Figure 17 displays the temperature difference over time between Cell 1 and the other two cells in a 1S3P battery pack tested without any cooling system. The y-axis represents the absolute temperature difference in degrees Celsius between each cell and Cell 1, which was consistently the hottest cell throughout the entire charge-discharge cycle. Specifically, the blue curve indicates the temperature difference between Cell 1 and Cell 2, while the green curve shows the difference between Cell 1 and Cell 3.

From the beginning of the test, both differences begin to rise, indicating Cell 1's higher surface temperature relative to the others. The blue line increases steadily and remains around 2 °C by the end of the cycle. In contrast, the green line rises more sharply, exceeding 6 °C at its peak.

This increasing thermal spread confirms a significant and growing temperature gradient between cells within the same parallel-connected pack.

The observed trend is attributed to internal resistance mismatches and pack geometry, where Cell 1—being physically closest to the electrical terminal—draws more current. This graph effectively visualizes the magnitude of thermal variation compared to the hottest cell (Cell 1) and shows how, without any cooling mechanism, thermal heterogeneity can become detrimental over time. Such gradients not only raise concerns about performance inconsistency but also about accelerated aging and potential safety risks in high-power applications if left unaddressed.

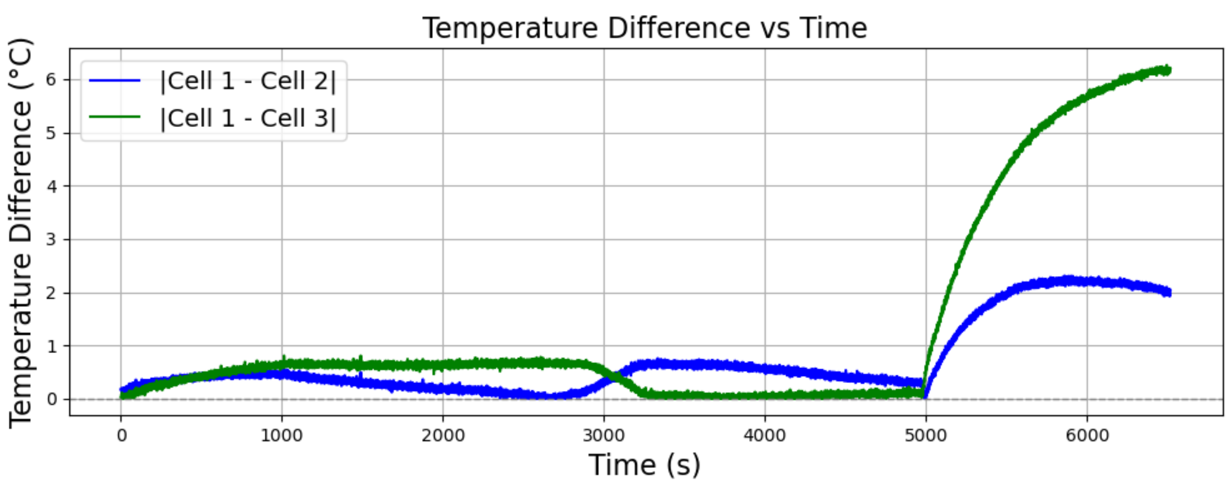

Figure 17 Cell Heterogeneity in 1S3P with no cooling

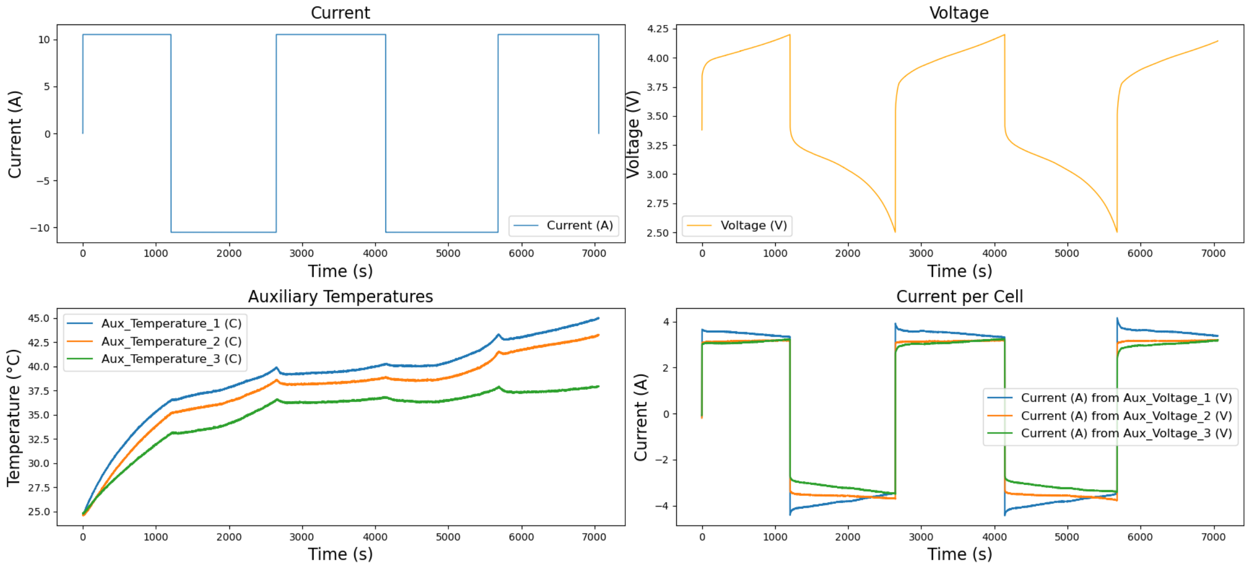

Figure 18 1S3P PCM Test Results

The 1S3P PCM cooled testing results demonstrated a noticeable improvement in the thermal behavior of the PCM-embedded battery pack compared to the pack without any cooling mechanisms. The PCM-enhanced pack was able to complete nearly three full charge-discharge cycles before reaching the upper-temperature threshold of 45°C. This indicates that the PCM effectively absorbed and redistributed heat, delaying excessive temperature rise.

Like the previous test, Cell 1 was the hottest temperature, followed by Cell 2, with Cell 3 maintaining the lowest temperature throughout the cycles. Notably, Cell 3 displayed an asymptotic thermal behavior, stabilizing around 37–38°C, which closely matches the melting point of the PCM used. This suggests that the PCM effectively regulated temperature by undergoing its phase transition, absorbing excess heat and preventing further temperature escalation in that region of the pack. However, despite this improvement, the cell still accumulated excessive heat, highlighting the need for additional strategies to achieve better temperature uniformity within the battery pack.

Figure 19 illustrates the temperature difference between Cell 1 and the other two cells over time for the 1S3P battery configuration embedded in Phase Change Material. As with the previous no-cooling test Figure 17, Cell 1 remains the hottest cell, and the temperature differences shown represent the magnitude of deviation in surface temperature relative to Cell 1. However, in this case, the magnitude of thermal differences is significantly reduced, suggesting that the PCM plays a major role in dampening thermal gradients.

Compared to the no-cooling scenario, where temperature differences reached over 6 °C between Cell 1 and Cell 3, the maximum difference in this PCM-cooled test appears to be contained below 4 °C for most of the cycle. While a gradual rise in temperature difference is still evident, the slope and magnitude are both notably lower than before. This outcome supports the effectiveness of PCM in absorbing and redistributing heat, especially during high-rate charge-discharge cycles.

Phase Change Materials are known for their latent heat absorption capacity, which allows them to buffer sudden temperature spikes by undergoing a phase transition. In this experiment, the PCM helped maintain safer, more uniform cell temperatures, reducing the risk of overheating and improving uniform thermal consistency across the pack. Although some heterogeneity remains, the thermal behavior has significantly improved, validating the inclusion of PCM as a passive thermal regulation strategy in compact battery systems.

This improvement is especially critical for ensuring cell longevity and pack safety, as uneven temperature profiles have been directly correlated with capacity fade and degradation acceleration in lithium-ion packs. Therefore, the observed reduction in inter-cell thermal deviation demonstrates that PCM is a viable option for reducing thermal mismatch in parallel-connected battery configurations.

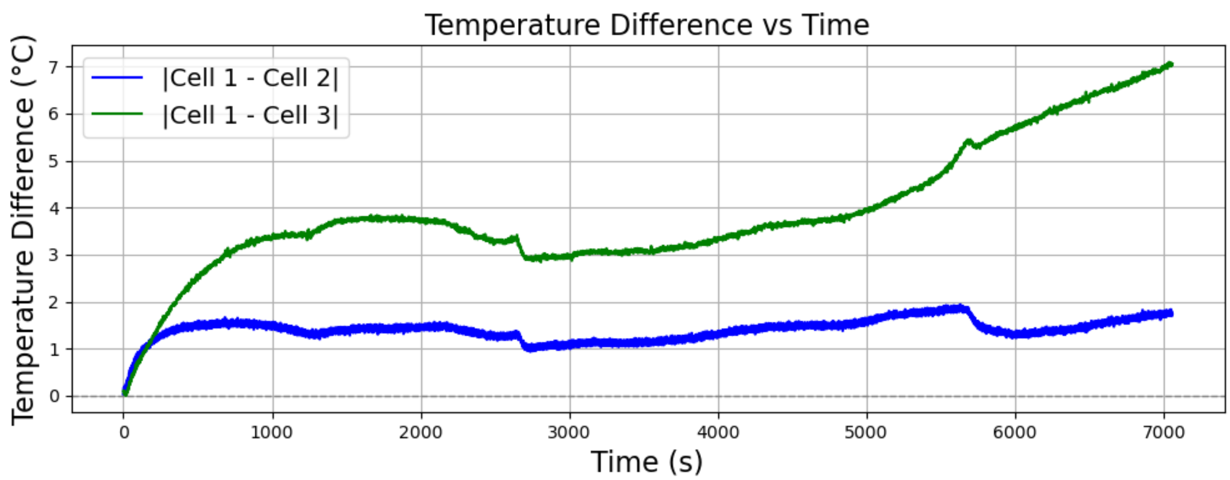

Figure 19 – Cell Heterogeneity in 1S3P with PCM

The next testing was conducted using a hybrid cooling setup, which combined both PCM and liquid cooling to evaluate its effectiveness in managing cell temperatures. The setup in Figure 11 and Figure 12 was implemented with an identical testing schedule as the previous two 1S3P tests.

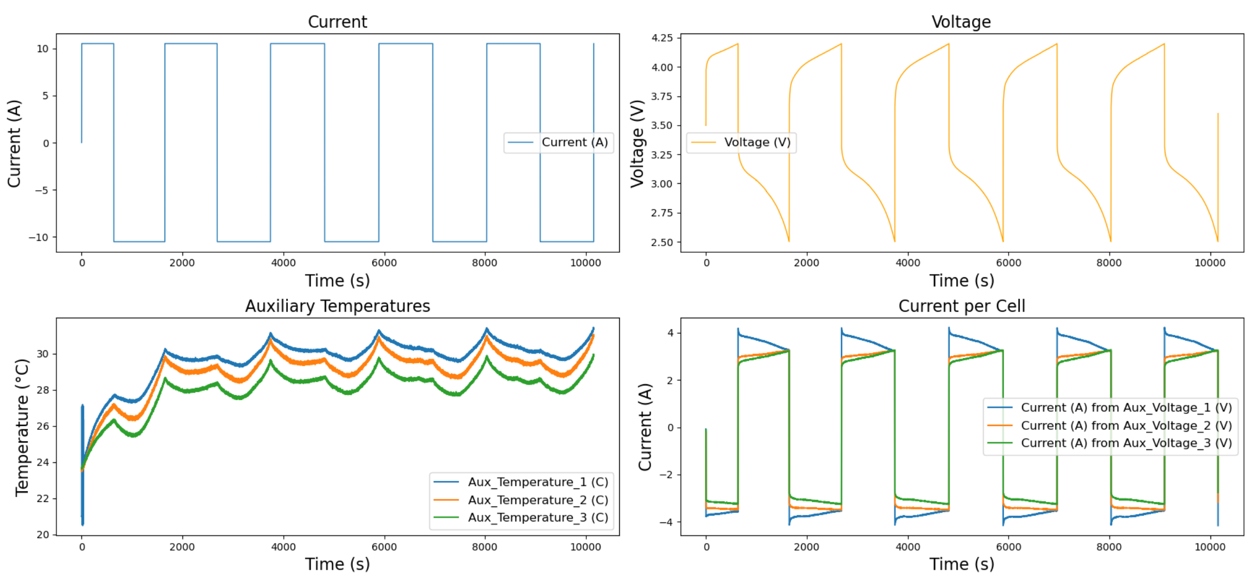

Figure 20 - 1S3P Hybrid Cooling

One key observation from this test is that the hybrid-cooled 1S3P battery pack, which integrates both PCM and water cooling, completed five full charge-discharge cycles without exceeding the 45°C temperature threshold. Unlike previous tests, where the pack temperature steadily increased until triggering the safety cutoff, the hybrid cooling system maintained a maximum temperature of only 32–33°C, demonstrating effective thermal regulation. The combination of PCM for passive heat absorption and water cooling for continuous heat dissipation effectively mitigated thermal buildup, allowing the pack to operate under high C-rates with enhanced temperature stability.

As with previous tests, Cell 1 remained the hottest, followed by Cell 2 and then Cell 3, maintaining a consistent thermal distribution pattern. However, a key difference observed in this test was that during the 4th and 5th cycles, the temperature profiles were nearly identical, indicating that the system had reached a steady-state thermal equilibrium. This suggests that the hybrid cooling system can sustain long-term thermal stability, preventing excessive temperature fluctuations over extended cycles. The combination of PCM and water cooling proved to be an effective and scalable solution for improving battery pack performance, longevity, and safety in high-power applications.

This result shows that the hybrid cooling system not only minimized temperature differences between cells but also provided stable thermal control over extended operation. The repeating charge-discharge cycles produced consistent thermal patterns, yet the cell-to-cell temperature difference remained under 2°C throughout the entire testing period. This suggests that the system was not merely delaying heat accumulation but actively managing and dissipating it in real-time.

The PCM layer absorbed latent heat during temperature spikes, reducing rapid thermal rises, while the liquid cooling loop continuously removed heat from the system, maintaining a low and stable average temperature. Because of this hybrid mechanism, the pack was not approaching any thermal runaway threshold or saturation point in the PCM, even during multiple cycles as shown in Figure 21.

As a result, the pack could have continued cycling the battery pack further, and the temperature profile would likely have remained similarly controlled. The system was operating in a steady thermal regime where both peak temperatures and temperature gradients were effectively regulated—making the hybrid BTMS a scalable and robust solution for long-term, high-power battery applications.

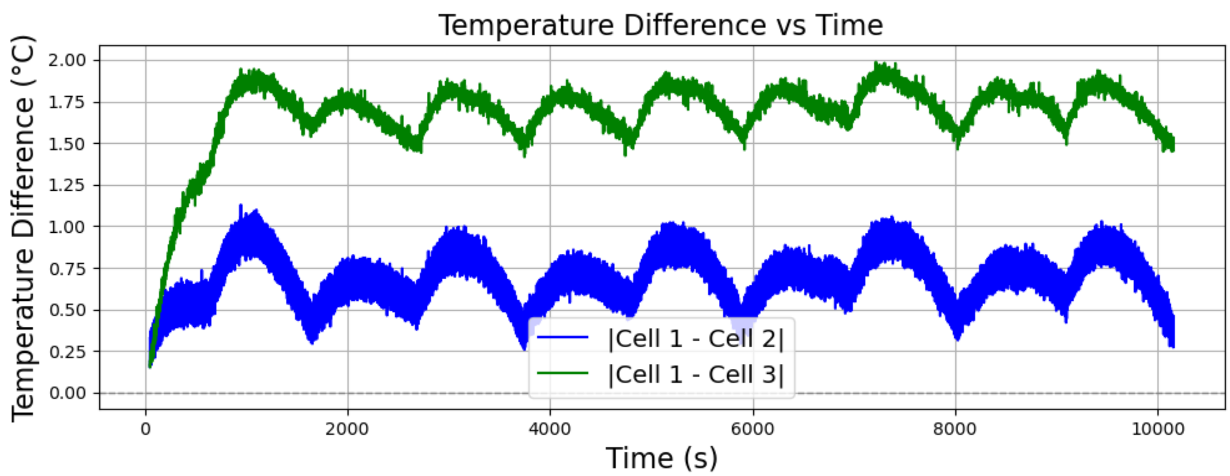

Figure 21 Cell Heterogeneity in 1S3P with Hybrid Cooling

Current Distribution within Pack

The current measurements per cell, calculated from shunt resistors using Ohms law, provided insight into cell-level behavior during charge-discharge cycles. In all test configurations, the cells did not receive an exactly equal current share, despite being in a parallel configuration. This discrepancy can be attributed to differences in internal resistance, which caused variations in current flow and heat generation.

Interestingly, in the hybrid cooling test, the current distributions among Cells 1, 2, and 3 remained more stable compared to the PCM-only test. This suggests that maintaining a lower and more uniform temperature may contribute to a more balanced current distribution, thereby improving overall pack efficiency and longevity.

Model

The physics model used for estimating the temperature profile of a lithium-ion battery cell is based on the first law of thermodynamics, which states that the change in internal energy of a system is equal to the net heat energy added to it. In this model, the temperature evolution of the battery is determined by the balance between heat generated from electrical resistance and heat dissipation to the surrounding environment.

The primary source of heat within the battery occurs due to the internal resistance of the cell. This is calculated by equation 4.

$$Q_{gen} = I^2 * R_{cell} \tag{4}$$

where I is the battery current and R is the resistance. This relationship follows Ohm's Law, where electrical power dissipated in a resistor is proportional to the square of the current. As a result, higher charging currents lead to exponentially greater heat generation, making thermal management particularly important in fast-charging applications.

The battery also loses heat to the surrounding environment, following Newton's Law of Cooling. This is expressed as

$$Q_{loss} = hA(T - T_{ambient}) \tag{5}$$

where h is the convective heat transfer coefficient, A is the battery surface area, and $T - T_{ambient}$ represents the temperature difference between the battery and ambient air. The value of h depends on the cooling mechanism, where natural convection results in lower heat dissipation, while forced air or liquid cooling significantly enhances cooling efficiency.

To determine the battery temperature at each time step, the model applies energy conservation, where the temperature change is calculated using equation 6.

$$dT = \frac{Q_{gen} - Q_{loss}}{mC_p} \tag{6}$$

where m is the battery mass and C_p is the specific heat capacity of the cell. This equation ensures that as heat accumulates, the battery temperature increases, and as heat dissipates, the battery temperature stabilizes or decreases.

Overall, this thermal model effectively predicts battery heating behavior during charging, allowing the evaluation of different charging strategies and cooling mechanisms. By incorporating these parameters, it can be used to optimize battery thermal management systems, prevent overheating, and extend battery lifespan in applications such as electric vehicles and energy storage systems.

Sensitivity Analysis

To understand the significance of each value in the physics mode a simple sensitivity analysis was conducted. In other words, this allows the identification of which parameter will impact the largest change in the temperature evolution of the battery cell. By applying sensitivity analysis to a PSO-based battery thermal model, researchers can prioritize the most critical parameters for optimization. If charging current and convection coefficient are found to be the most sensitive variables, the model can focus on dynamically adjusting the charge rate and cooling system settings rather than overcomplicating the optimization with less influential parameters. Ultimately, sensitivity analysis enhances model accuracy, reduces computational complexity, and provides valuable insights for improving battery performance, safety, and longevity.

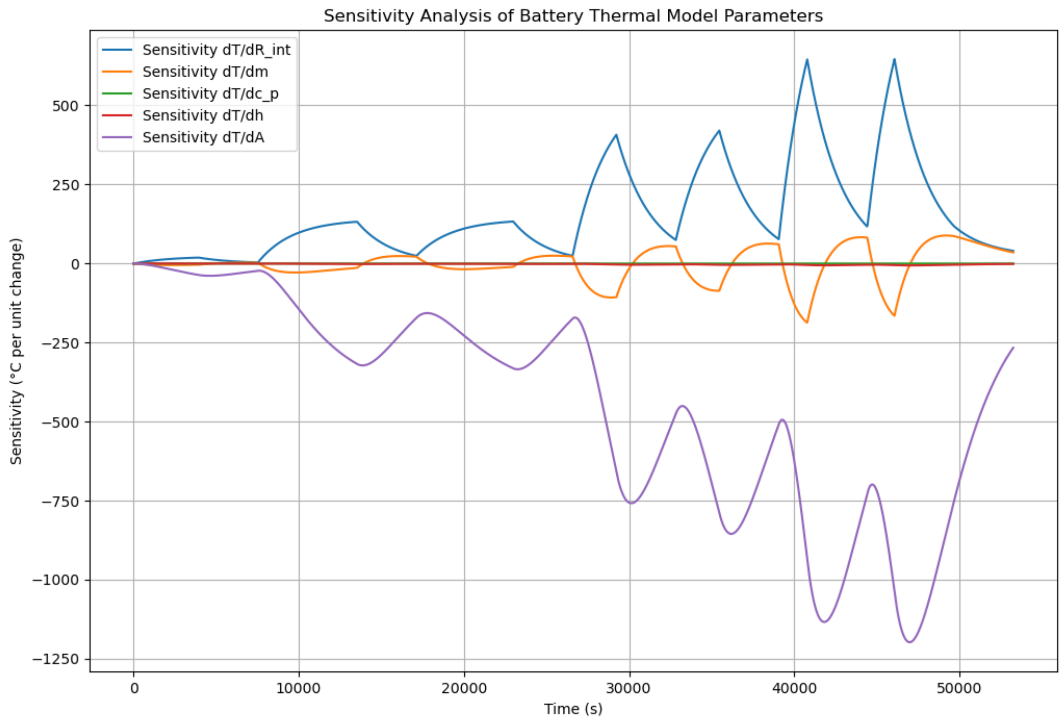

Figure 22 Sensitivity Analysis

One of the most dominant factors affecting temperature rise is internal resistance, as seen in the oscillations of its sensitivity curve. The peaks in sensitivity correlate with high current discharge events, indicating it is the primary cause of temperature spikes. This finding underscores the importance of minimizing internal resistance through improved electrode materials, better manufacturing consistency, and optimized charge-discharge protocols to prevent excessive heating, particularly under high-power operation.

Conversely, the sensitivity of battery mass and specific heat capacity remains relatively small and stable, showing these parameters have a minimal influence on battery temperature fluctuation. While increasing mass or heat capacity can slightly slow down the temperature rise, it does not significantly prevent overheating. This suggests that heat dissipation, rather than heat storage, is a more effective cooling strategy for lithium-ion batteries.

The sensitivity of the convective heat transfer coefficient is also relatively low, meaning that air cooling alone is not sufficient to control temperature spikes. Even with improved airflow, the cooling effect is limited, especially in high C-rate charging and discharging scenarios. This reinforces the need for hybrid cooling strategies, such as combining convection with liquid cooling and phase change materials.

Among all parameters, the surface area has the strongest negative sensitivity, meaning that increasing the battery's heat-dissipating surface area is one of the most effective ways to lower temperature. The large fluctuations in sensitivity suggest that during cycles, expanding surface area significantly improves cooling efficiency. This highlights the importance of battery pack design, where incorporating thermal spreaders, and extended cooling fins can greatly enhance heat dissipation and maintain lower operating temperatures.

In conclusion, internal resistance and surface area are the two most critical parameters affecting battery temperature. Reducing resistance minimizes heat generation while increasing surface area improves heat dissipation. Simply increasing battery mass or heat capacity is not sufficient for thermal regulation, and forced convection alone does not provide adequate cooling under high-power conditions. These findings emphasize the need for low-resistance battery materials, efficient thermal interfaces, and hybrid cooling solutions to ensure safe and optimal battery performance in high-power applications such as electric vehicles and energy storage systems.

Py Swarm Optimization (PSO)

Particle Swarm Optimization (PSO) was used to calibrate a simplified physics-based thermal model for an 18650 lithium-ion cell during the single cell charging cycle. Due to modeling constraints and practical limits, the simulation focused exclusively on the charging phase at three C-rates: 0.5C, 1C, and 1.5C, rather than modeling full charge-discharge cycles. Each C-rate was modeled independently to account for variations in battery behavior at different current levels.

In PSO, each particle represents a candidate solution—in this case, a set of thermal model parameters:

$$Particle = Set\ of\ Parameters: [R_{int},\ h]$$

where R_{int} is the internal resistance of the battery and h is the convective heat transfer coefficient. These two parameters were selected as the variables to optimize because they are most sensitive to changes in current and significantly impact temperature rise during charging.

The parameters for surface area (A = 0.0123 m²) and mass (m = 0.0485 kg) were fixed based on manufacturer specifications. The specific heat capacity (c_p) of the cell was set to 1100 J/kg·K based on values reported in a study from the University of Waterloo, which analyzed the thermal behavior of cells under various operational conditions [33].

The PSO algorithm updates the velocity and position of each particle based on its best-known position and the global best across all particles using equations 6 and 7.

$$Velocity\ Update:\ v_j^{t+1} = w \cdot v_j^t + c_1 r_1 \left(p_{best,j} - x_j^t\right) + c_2 r_2 \left(g_{best,j} - x_j^t\right) \tag{6}$$

$$Position\ Update: x_j^{t+1} = x_j^t + v_j^{t+1} \tag{7}$$

This enables particles to explore and converge toward the optimal set of parameters.

The objective function to be minimized is the mean squared error (MSE) between the simulated and measured temperatures, show in equation 8.

$$\text{Error is measured by MSE} = \frac{1}{n}\sum_{i=1}^{n}(T_i - \hat{T}_i)^2 \quad (8)$$

where T_i is the experimentally measured temperature and $\hat{T}_i$ is the simulated model output. The MSE quantifies how well the model replicates the real-world thermal behavior of the cell during charging.

By minimizing the MSE through PSO, the optimized values of R_{int} and h for each C-rate were identified, enabling accurate modeling of the temperature profile. This process ensures the model remains physically interpretable while maintaining flexibility and adaptability to different C-rates.

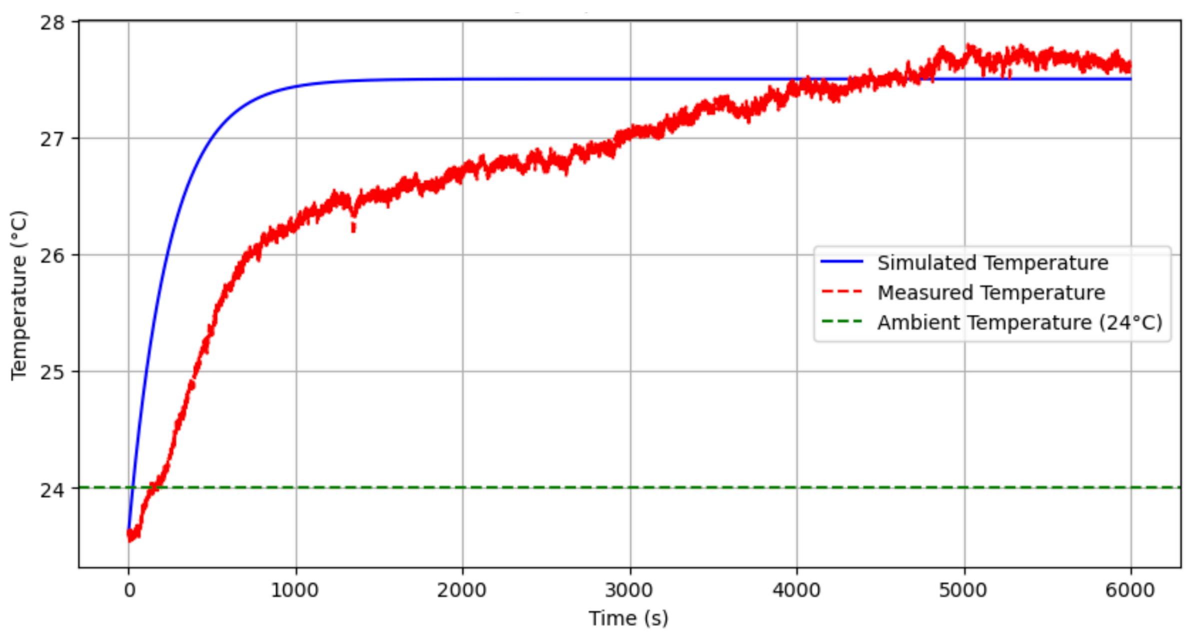

Figure 23 0.5C Model

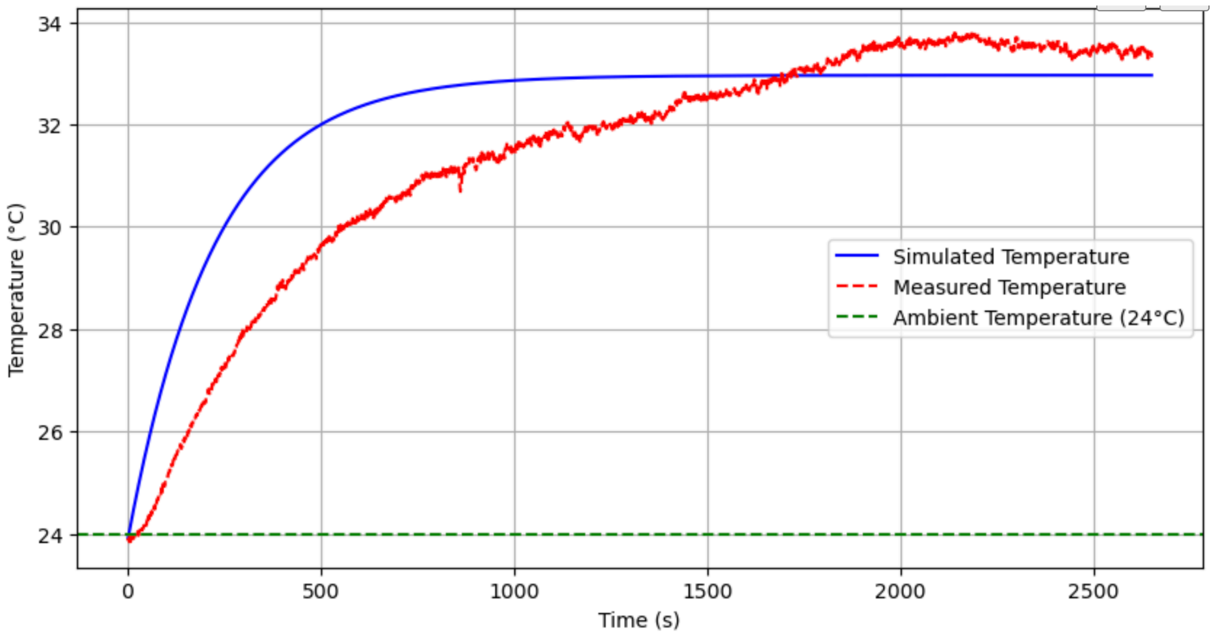

Figure 24 1C Model

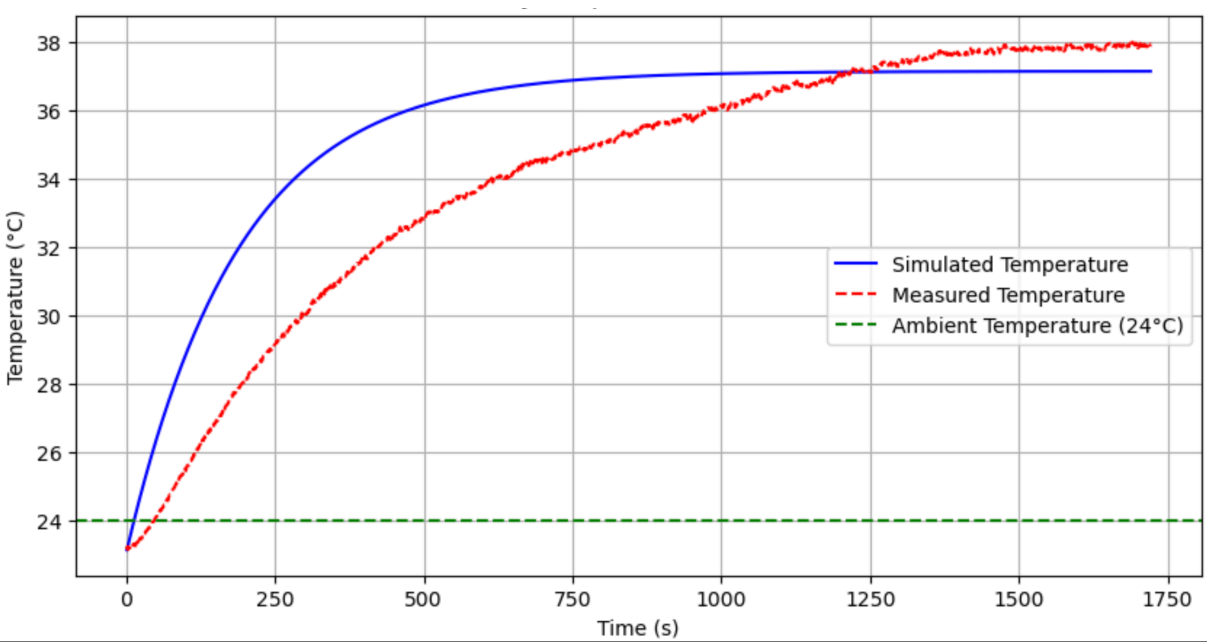

Figure 25 1.5C Model

Table 2 Summary of Simulated Parameters

	0.5C	1C	1.5C
Internal Resistance (R_{int}) (Ω)	1.11	0.78	0.69
Heat Transfer Coeff (h) (W/m²·K)	18.16	19.94	23.57
Area (A) (m²)	0.0123	0.0123	0.0123
Mass (m) (Kg)	0.0485	0.0485	0.0485
Specific Heat (c_p) (J/kg·K)	1100	1100	1100
MSE	0.538	0.892	2.532

As observed from the table above, there are clear trends in how battery parameters vary with different C-rates. One of the most significant trends is the decrease in internal resistance as the C-rate increases. This is expected, as higher charge currents facilitate the transport of more lithium ions within the electrolyte, effectively reducing the cell's electrical impedance. However, despite the lower internal resistance, the overall heat generation still increases due to the squared dependence on current, as described by Joule's Law. While a lower resistance reduces the voltage drop across the battery, it does not prevent excessive heating, showing the importance of thermal management strategies at higher C-rates.

Another noticeable trend is the increase in the heat transfer coefficient with increasing C-rate. This suggests that the battery generates more heat at higher charge rates, allowing for greater heat dissipation. However, the improvement in convective heat transfer is not sufficient to fully offset the rapid heat generation at high C-rates, which indicates that additional cooling mechanisms such as forced air cooling, liquid cooling, or phase change materials may be necessary to prevent thermal runaway.

The battery's surface area and mass remained nearly constant across all C-rates, reflecting real-world constraints where the physical dimensions of a battery do not change. To mimic realistic conditions, the model applied strict boundaries to prevent unrealistic changes in mass and surface area. This decision was based on sensitivity analysis results, which demonstrated that mass and area can significantly impact temperature fluctuations. Allowing them to change freely in an optimization model would create artificial scenarios where cooling is improved due to increased mass or expanded surface area, which is not practical in real applications.

Conclusion

This study explored the thermal behavior of batteries through both physical testing and computational modeling, focusing on the impact of C-rate variations and different cooling strategies on battery temperature regulation. The physical testing phase involved charging and discharging 18650 cells under different C-rates while measuring surface temperature, voltage, and current. The results confirmed that higher C-rates significantly increased heat generation, with temperature rising due to Joule heating and internal resistance effects.

To mitigate overheating, two different cooling strategies were tested. Phase Change Material and hybrid cooling. The PCM system effectively delayed temperature rise in the initial charge cycles. However, at higher C-rates, the PCM's thermal capacity became saturated, leading to noticeable temperature spikes as heat accumulated over time. In contrast, the hybrid system exhibited a much more stable thermal profile, where the battery temperature never exceeded safety limits. The hybrid system demonstrated asymptotic behavior, meaning that as heat was generated, it was continuously dissipated at a sufficient rate, preventing uncontrolled temperature rise and consistent temperature profile. This result confirms that active cooling methods are far more effective than passive PCM cooling for sustained high-power applications.

Building on the experimental findings, a physics-based thermal model was developed to predict battery temperature behavior under different operating conditions. The thermal model incorporated key physical parameters, such as internal resistance, heat transfer coefficient, mass, surface area, and specific heat capacity, to estimate temperature rise accurately. Sensitivity analysis revealed that internal resistance and surface area were the dominant factors affecting battery temperature, emphasizing the importance of low-resistance battery designs and enhanced cooling configurations. Additionally, the model showed that while higher C-rates improved convective heat transfer efficiency, passive cooling alone was insufficient for maintaining stable temperatures, especially during high C-rates.

An important aspect highlighted through this study is the presence of thermal heterogeneity among cells within a battery pack, especially under high C-rate conditions. Experimental results consistently showed that cells positioned closer to the terminal experienced higher temperatures, leading to noticeable temperature gradients across the pack. This non-uniform temperature distribution can cause accelerated aging in the hotter cells, reduced overall pack efficiency, and increased risk of thermal runaway. While PCM offered partial thermal buffering, it was insufficient in maintaining uniformity. However, the hybrid cooling system demonstrated a significant reduction in cell-to-cell temperature variation, keeping the differential within 2°C.

As lithium-ion battery technology continues to evolve, future research should focus on real-time adaptive cooling strategies, machine learning-driven thermal optimization, and advanced materials for improved heat dissipation. These advancements will be critical for ensuring safe, efficient, and reliable battery operation, particularly in demanding applications such as electric vehicles, aerospace systems, and large-scale energy storage.

Future Works

Due to constraints, certain aspects of this research were not fully explored. In the experimental phase, one significant area for future work is testing a larger battery pack. While this study successfully examined a 1S3P battery configuration, expanding the testing to a 3S3P pack or larger would provide a deeper understanding of how cells behave collectively under different charge and discharge rates. This would allow for a more comprehensive analysis of thermal properties, cell balancing, and inter-cell heat distribution in the configurations. However, one of the primary limitations encountered was battery tester capacity. The available testing equipment had voltage and current constraints, making it impractical to test higher-capacity packs under realistic operating conditions. Future research should explore higher-capacity battery testers or modular testing setups that can accommodate larger packs.

Additionally, for the 1S3P pack, further testing could involve placing the system in a thermal chamber to study its behavior under different ambient temperature conditions. While the cooling mechanisms performed well in standard ambient conditions, it is crucial to determine the upper threshold of effectiveness by testing at elevated temperatures to assess performance in a more realistic outdoor temperature. This would be particularly relevant for applications in electric vehicles, where batteries are often exposed to varying thermal conditions. Another experimental extension would be testing different battery cell formats, such as 21700 cells, which are larger than 18650 cells and have different thermal properties due to their higher energy density. Conducting the same thermal tests on different cell types would help generalize the findings and determine how battery size affects thermal behavior and cooling efficiency.

For the computational modeling, due to time constraints, the developed thermal model was limited to the charge portion of a single cell. One major improvement would be to extend the model to include the discharge cycle, which exhibits different thermal characteristics. While the lumped thermal model used in this study was beneficial for quick estimations with low computational cost, it has limitations, such as not capturing spatial temperature variations and being less accurate for discharge modeling.

Future work could explore more advanced modeling techniques such as Finite Element Analysis or Machine Learning-based models. FEA modeling would allow for highly detailed and spatially accurate thermal simulations, providing insights into temperature gradients within the cell and battery pack. However, FEA is computationally intensive and may not be suitable for real-time applications. On the other hand, machine learning models could leverage historical temperature data to develop predictive analytics for battery thermal behavior. While ML models can capture complex and nonlinear thermal trends, they require large amounts of training data, which necessitates extensive experimental testing to build a reliable dataset.

In summary, future research should focus on scaling up battery pack testing, exploring different cell chemistries and sizes, improving environmental testing conditions, and advancing computational modeling techniques. Combining physics-based models with machine learning-driven predictive models could lead to more accurate and efficient Battery Thermal Management Systems, improving battery safety, longevity, and overall performance in high-power applications.

Acknowledgement

I would first like to express my sincere gratitude to my thesis chair, Dr. Zhang Dong, for his continuous support, insightful guidance, and encouragement throughout this research. His mentorship was instrumental in shaping the direction of my work and helping me navigate the challenges of both experimentation and modeling. I am truly thankful for his patience and dedication during each stage of this thesis.

I would also like to extend my appreciation to my committee members, Dr. Merchan Merchan and Dr. Xu, for their time, thoughtful feedback, and valuable suggestions that helped refine and strengthen this thesis. Their input contributed greatly to the quality and depth of my final work.

I am grateful to the team at Dr. Garg's lab for their assistance in providing the phase change material and supporting the preparation and handling process. Their help was essential in carrying out the cooling system experiments accurately and efficiently.

Special thanks to the University of Oklahoma's Innovation Hub, where I had the opportunity to work during my graduate studies. The experience enhanced my skills in prototyping and fabrication and gave me access to equipment that greatly aided in building custom battery enclosures.

Reference

[1] J. luqman, “Greenhouse gases utilization: A review,” *ELSEVIER*.

[2] “Alternative Fuels Data Center: Electric Vehicle Benefits and Considerations.” Accessed: Jan. 31, 2025. [Online]. Available: https://afdc.energy.gov/fuels/electricity-benefits

[3] “Electric Vehicles - Worldwide | Statista Market Forecast,” Statista. Accessed: Jan. 31, 2025. [Online]. Available: https://www.statista.com/outlook/mmo/electric-vehicles/worldwide

[4] “Vermont Laws.” Accessed: Jan. 31, 2025. [Online]. Available: https://legislature.vermont.gov/statutes/section/23/001/00004

[5] Z. Xianlai, “Solving spent lithium-ion battery problems in China: Opportunities and challenges”.

[6] A. Etengoff, “How do EV battery cell charge and discharge rates compare?,” EV Engineering & Infrastructure. Accessed: Feb. 04, 2025. [Online]. Available: https://www.evengineeringonline.com/how-do-ev-battery-cell-charge-and-discharge-rates-compare/

[7] S. K. Maknikar and A. M. Pawar, “Application of phase change material (PCM) in battery thermal management system (BTMS): A critical review,” *Mater. Today Proc.*, Aug. 2023, doi: 10.1016/j.matpr.2023.08.329.

[8] A. Dinker, M. Agarwal, and G. D. Agarwal, “Heat storage materials, geometry and applications: A review,” *J. Energy Inst.*, vol. 90, no. 1, pp. 1–11, Feb. 2017, doi: 10.1016/j.joei.2015.10.002.

[9] B. Zhang, “Numerical investigation of lithium-ion battery thermal management system performance influenced by physical properties of PCM”.

[10] N. Kumar, “Performance assessment of PCM-based cooling in electric vehicle battery packs compared to conventional methods”.

[11] S. Li, C. Zhang, Y. Zhao, G. J. Offer, and M. Marinescu, “Effect of thermal gradients on inhomogeneous degradation in lithium-ion batteries,” *Commun. Eng.*, vol. 2, no. 1, pp. 1–14, Oct. 2023, doi: 10.1038/s44172-023-00124-w.

[12] T. Rüwald *et al.*, “Experimental investigation of cell degradation in packs of parallel-connected cells under different temperature distributions,” *J. Energy Storage*, vol. 104, p. 114427, Dec. 2024, doi: 10.1016/j.est.2024.114427.

[13] F. Liu, Q. Yang, D. Zheng, W. Qin, X. Cheng, and J. Li, “A novel battery thermal management system with air–liquid coupled cooling based on particle swarm optimization,” *Appl. Therm. Eng.*, vol. 271, p. 126391, Jul. 2025, doi: 10.1016/j.applthermaleng.2025.126391.

[14] Y.-H. Lin, M.-T. Lee, and Y.-H. Hung, “A thermal management control using particle swarm optimization for hybrid electric energy system of electric vehicles,” *Results Eng.*, vol. 21, p. 101717, Mar. 2024, doi: 10.1016/j.rineng.2023.101717.

[15] “Panasonic NCR18650B 3400mAh 4.9A Battery,” 18650BatteryStore.com. Accessed: Apr. 30, 2025. [Online]. Available: https://www.18650batterystore.com/products/panasonic-ncr18650b

[16] “The Widely Applications of 18650 Batteries.” Accessed: Apr. 30, 2025. [Online]. Available: https://www.lithium-polymer-battery.net/the-widely-applications-of-18650-batteries/

[17] “Panasonic NCR18650B 3350mAh 4.87A Battery,” IMR Batteries. Accessed: Feb. 04, 2025. [Online]. Available: https://imrbatteries.com/products/panasonic-ncr18650b-3350mah-4-87a-battery

[18] “NCR18650B 3400mAh Li-ion Battery,” Fly High FPV. Accessed: Apr. 22, 2025. [Online]. Available: https://flyhighfpv.com/products/ncr18650b-3400mah-li-ion-battery

[19] *This Is How Solid Power Manufactures Its Solid-State Batteries*. Accessed: Apr. 30, 2025. [Online Video]. Available: https://motorsport.tv/embed/URYzpI3S?edition=ev%2Fev_us&mstv_player_position=embed

[20] “Tesla Model S Battery System: An Engineer’s Perspective.” Accessed: Feb. 04, 2025. [Online]. Available: https://circuitdigest.com/article/tesla-model-s-battery-system-an-engineers-perspective

[21] “Tesla Model S Battery System: An Engineer’s Perspective.” Accessed: Apr. 22, 2025. [Online]. Available: https://circuitdigest.com/article/tesla-model-s-battery-system-an-engineers-perspective

[22] “Why Nickel Strips Are Ideal for Battery Packs.” Accessed: Apr. 30, 2025. [Online]. Available: https://cellsaviors.com/blog/why-use-nickel-strips-for-battery-packs

[23] “AWithZ 14.6 KW Capacitor Battery Spot Welder, Spot Welder 3-in-1 Auto, manual, Foot Pedal Three Modes Battery Farad Welding Equipment for 18650/LiFePO4 Lithium Battery Pack Building - Amazon.com.” Accessed: Apr. 22, 2025. [Online]. Available: https://www.amazon.com/AWithZ-Capacitor-Battery-Equipment-Building/dp/B0DRBTS2X7/ref=sr_1_43?crid=1BJQ1DAYPWFKC&dib=eyJ2IjoiMSJ9.FAePoZXjHt6XLL1F6nD-4QCD0tXqyjgfIIba6SkSZXxR-7EWHZnjdAUhcdFDoobDOzP-nVZVsONWZWFHez2Ylmx4VJD2zJeEFzMKhJAyjAhIA5jERxKkel8c4hhZgRzo6Ar0YwDCPQv3a0st9UL7j9fezqAENSmndMztLDEPPwhlWzEKBZ2EuSsNWqPrpHQPHvAWaoztvgNrpm7Q2ialnxNhSEtg-PAapEQuhU_xvqjyht9DK0KT851BBkd39z-grY15FbpcEdPZX2Yn09pgQcss5eYxXCpHZBZQbn2Vlx4.DqryzkQeZccGM9uwqaoKZ4QEokxot5O69g_KuQ6kKV8&dib_tag=se&keywords=battery+spot+welder&qid=1745371369&sprefix=battery+spot+weld%2Caps%2C268&sr=8-43

[24] J. Kim, J. Oh, and H. Lee, “Review on battery thermal management system for electric vehicles,” *Appl. Therm. Eng.*, vol. 149, pp. 192–212, Feb. 2019, doi: 10.1016/j.applthermaleng.2018.12.020.

[25] R. A. Lawag and H. M. Ali, “Phase change materials for thermal management and energy storage: A review,” *J. Energy Storage*, vol. 55, p. 105602, Nov. 2022, doi: 10.1016/j.est.2022.105602.

[26] J. Luo, “Battery thermal management systems (BTMs) based on phase change material (PCM): A comprehensive review”.

[27] Y. Ding, H. Ji, M. Wei, and R. Liu, “Effect of liquid cooling system structure on lithium-ion battery pack temperature fields,” *Int. J. Heat Mass Transf.*, vol. 183, p. 122178, Feb. 2022, doi: 10.1016/j.ijheatmasstransfer.2021.122178.

[28] M. J. Koshkouei, N. Fereshteh Saniee, and A. Barai, “Thermocouple selection and its influence on temperature monitoring of lithium-ion cells,” *J. Energy Storage*, vol. 92, p. 112072, Jul. 2024, doi: 10.1016/j.est.2024.112072.

[29] G. Srivastava, R. Nandan, and M. K. Das, “Thermal runaway management of Li ion battery using PCM: A parametric study,” *Energy Convers. Manag. X*, vol. 16, p. 100306, Dec. 2022, doi: 10.1016/j.ecmx.2022.100306.

[30] “Thermaltake T1000 Coolant- Pure Clear,” Thermaltake USA. Accessed: Apr. 30, 2025. [Online]. Available: https://thermaltakeusa.com/products/thermaltake-t1000-coolant-pure-clear-cl-w245-os00tr-a

[31] S. Rana, “Lithium-ion battery thermal management system using MWCNT-based nanofluid flowing through parallel distributed channels: An experimental investigation”.

[32] W. Shen, N. Wang, J. Zhang, F. Wang, and G. Zhang, “Heat Generation and Degradation Mechanism of Lithium-Ion Batteries during High-Temperature Aging,” *ACS Omega*, vol. 7, no. 49, pp. 44733–44742, Dec. 2022, doi: 10.1021/acsomega.2c04093.

[33] O. Lazarenko, O. Pazen, Y. Velykyi, R. Parkhomenko, and Y. Stepaniak, “Determination of Thermal Physical Characteristics of the Panasonic NCR18650b Lithium-Ion Power Supply Element,” *Proc. Latv. Acad. Sci. Sect. B Nat. Exact Appl. Sci.*, vol. 78, no. 5–6, pp. 372–379, Dec. 2024, doi: 10.2478/prolas-2024-0047.